Boundary-Layer Meteorol (2016) 161:335–353
DOI 10.1007/s10546-016-0172-7

RESEARCH ARTICLE

# PM10 Emission, Sandblasting Efficiency and Vertical Entrainment During Successive Wind-Erosion Events: A Wind-Tunnel Approach

**J. E. Panebianco**[1] · **M. J. Mendez**[1,2] · **D. E. Buschiazzo**[1,2,3]

Received: 1 August 2015 / Accepted: 24 May 2016 / Published online: 16 June 2016


**Abstract** A wind-tunnel experiment was carried out to measure saltation and PM10 (particulate matter with a mean aerodynamic diameter less than 10 μm) emission during three successive wind-erosion events on three different surfaces: an unpaved road and two different textured agricultural soils: a sandy loam and a loamy sand. The total horizontal mass transport ($Q$) and the PM10 emissions ($E$), were measured at two friction velocities: 0.2 and 0.3 m $s^{-1}$. Results indicated that $Q$ decreased rapidly in time over all surfaces, as the $Q$ values were only 13–17 % of the amount registered during the first event. Similar trends were detected at both wind speeds. However, $E$ values showed a lower relative decrease in the second wind-erosion event at the lower wind speed (25–51 % of the initial amounts) than at the higher wind speed (19–28 % of the initial amounts) over all surfaces. After the second wind-erosion event, both $Q$ and $E$ values remained constant except for the unpaved road, where both values decreased by 50 % in relation to the second event. Emission from the agricultural soils was sustained over successive wind-erosion events even when saltation was low. The sandblasting efficiency for PM10 emission was found to be higher for agricultural soils than for the unpaved road, and increased over wind-erosion events particularly in agricultural soils, and this was also reflected in the PM10 vertical entrainment. Results suggest that sandblasting efficiency and PM10 vertical distribution can change among wind-erosion events even for the same surface. The saltation fraction to PM10 content ratio can be a simple indicator of the general behaviour of an emitting surface during successive wind-erosion events.

**Keywords** PM10 emission · Sandblasting efficiency · Vertical entrainment · Wind erosion · Wind speed

✉ J. E. Panebianco
juanpanebianco@yahoo.com

1 Instituto de Ciencias de la Tierra y Ambientales de La Pampa (INCITAP, CONICET-UNLPam), Santa Rosa, La Pampa, Argentina

2 Universidad Nacional de La Pampa (UNLPam), Santa Rosa, La Pampa, Argentina

3 Instituto Nacional de Tecnología Agropecuaria (INTA), Anguil, La Pampa, Argentina

## 1 Introduction

PM10 is defined as particulate matter with a mean aerodynamic diameter less than 10 μm. Wind erosion and fine particulate matter (PM10) emissions are linked processes that can affect the Earth and atmosphere in numerous ways. The amount of PM10 emissions in the atmosphere is particularly important for human health (Dockery and Pope 1994; Carvacho et al. 2006) and for processes related to the long range translocation of nutrients and atmospheric radiation (Harrison et al. 2001; McTainsh and Strong 2007). Agricultural lands (Kjelgaard et al. 2004; Zobeck and Van Pelt 2006) as well as unpaved roads (Goossens and Buck 2011) are potential dust sources in arid and semi-arid regions of the world. In the centre of Argentina, semi-arid conditions with poorly aggregated soils, high precipitation variability and high wind speeds are frequent. Agricultural and human activity in these areas has produced accelerated wind erosion of soil (Buschiazzo et al. 1999), while unpaved roads extend in total more than 17,000 km in length, even considering only the area of La Pampa province (143,440 $km^2$). This region is affected by both the anticyclone of the Pacific Ocean and the anticyclone of the Atlantic Ocean. Hence, dust and PM10 emissions from this area could be transported to nearby agricultural regions and ecosystems as well as distant continental areas and even to the Atlantic Ocean (Mahowald et al. 2005).

PM10 emission has been related to the clay content of the surface (Marticorena and Bergametti 1995) and to clay and organic matter content (Aimar et al. 2012). But other authors have also found that surfaces with poor silt content can be large emitters (Sweeney et al. 2011). The suspension component can also be important in loessic soils (Sharratt et al. 2007), and it is known that the length of time under high wind conditions has an effect on the PM10 emission rate on disturbed soils (Baddock et al. 2011). Dust emission from unpaved roads has also been studied (Etyemezian et al. 2003; Goossens and Buck 2009), although road studies are mainly focused on vehicle-generated dust and not on wind-induced processes. Unpaved roads can be considered one of the most important dust sources in some regions, especially roads that are oriented along the predominant wind direction.

A major challenge in understanding the link between dust production and wind erosion is that many parameters vary independently in space and time (Alfaro and Gomes 2001; Shao 2008). PM10 emissions have been estimated using wind tunnels over agricultural soils (Aimar et al. 2012), playas (Roney and White 2006) and mine tailings (McKenna Neuman et al. 2009). However, there are few measurements of the PM10 to total sediment flux proportion, and even less is known about the behaviour of these in successive storms, or during continuous wind-blowing conditions. It is known that time-integrated processes involving the soil mass flux and related issues are complex, especially at the field scale (Kjelgaard et al. 2004). McKenna Neuman et al. (2009) identified the difficulties of working with a time-changing process under wind-tunnel conditions. Houser and Nickling (2001a) concluded that time-dependant processes can affect the relationship between PM10 emission and velocity shear. Liu et al. (2003) studied the short-term dynamics of soil wind erosion and determined that the diameter of the eroded soil particle became smaller with increasing wind duration. López (1998) determined that estimations obtained from dust-emission models deviate from measurements because of the changes in the erosion emission process with time. Alfaro et al. (1998) discussed the importance of the ratio of the PM10 emission flux to the saltating particle flux (called sandblasting efficiency) for dust-production modelling, but did not consider the possible changes of this parameter in successive wind-erosion events. In a very recent study, the length of the measurement period was also mentioned as a source

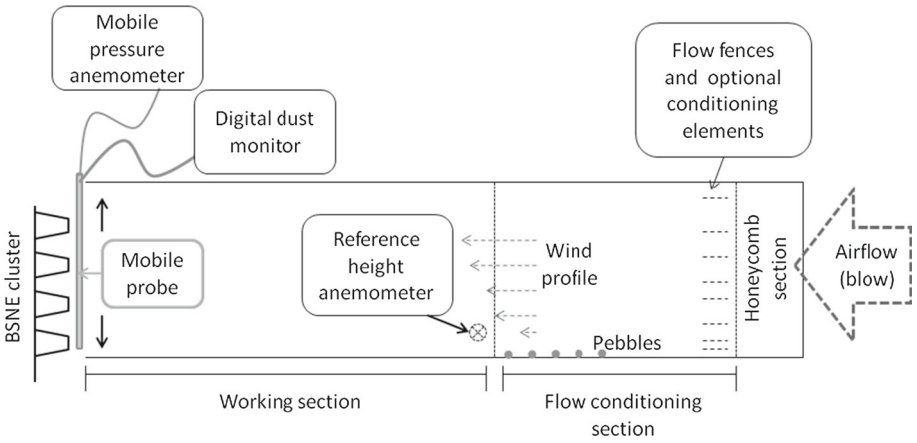


**Fig. 1** The wind-tunnel facility. Dimensions are provided in the text

of uncertainty in the relation between the horizontal mass flux and the PM10 flux (Whicker et al. 2014).

The objective of the present work is to determine how wind speeds and successive wind-erosion events affect wind erosion, PM10 emission and the sandblasting efficiency of three different sandy surfaces.

## 2 Materials and Methods

### 2.1 The Wind Tunnel

The wind tunnel has an overall length of 9 m and the working section is 6 m long, 1 m high and 0.5 m wide, see Fig. 1. Air is blown into the wind tunnel by means of a 1-m diameter propeller attached to a Honda GX 670 engine that is located on top of a portable chassis, and has a power of 15.3 kW. The air moved by the propeller is driven towards a descending curved section (not shown in Fig. 1), leading to a horizontal movement at ground level. Before entering the working section the air flows through a 0.5-m long honeycomb section (196 holes of 58 × 35 mm each), and the flow then enters a conditioning section, which is 2 m long, and that allows the installing of optional and replaceable elements. The floor of this section is completely covered by galvanized metal and it has eight 0.2-m wide horizontal deflectors that can be adjusted for modifying the airflow, and roughness elements in the form of pebbles can be distributed optionally. Additionally, an abrader hopper can be used for introducing saltating particles. Flow conditioning sections are necessary before the testing or working section of every boundary-layer wind tunnel (Van Pelt et al. 2010). Finally, the section of the wind tunnel where the wind stress over the surface is simulated is 4 m long and has a bare floor on which to place the soil samples.

### 2.2 Soil Characteristics

Surface samples were taken from the first 0.025 m of two agricultural soils: a loamy sand (LS), a sandy loam (SL), and from a sandy unpaved road (UR) from near Santa Rosa in

the central semi-arid Pampas of Argentina (36°46″S latitude, 64°16″W longitude and 210 m.a.s.l.). Soil samples were placed in plastic bags to carry the soil from the field to the laboratory.

Particle-size distribution analysis was made by means of a Malvern Mastersizer 2000 laser analyzer. Table 1 shows the results classified according to the expected wind-transport mechanism for each particle size. For dispersing the particles to some extent, samples were analyzed by removing the organic matter; this removal is part of the traditional particle-size analysis used in soil classification (Gee and Bauder 986) and is useful in determining the proportion of grains present in the soil. We call this the high dispersion analysis. The analysis without eliminating the organic matter is more related to the proportions of the aggregates that are naturally present in the soil and that are available to be transported by the wind. We call this the low dispersion analysis. The last row in Table 1 indicates the ratio of the saltation fraction to PM10 concentration, which quantifies the amount of PM10 available within the saltation fraction.

Experimental conditions of the soil samples are shown in Table 2. Organic matter content was determined by wet combustion (Walkley and Black 1934), and the erodible fraction of the dry aggregate stability, as well as the aggregate size distribution of each sample, were determined by means of a rotary sieve (Fyrear Fryrear (1985), Fig. 2).

Agricultural soils were tilled with a double disk, 15 days before the sampling, and further sample alteration occurred during sampling and transport. Hence, the soil samples were very disturbed. The unpaved road was very loose, and had no signs of compaction. In the laboratory, the soil samples were passively dried outdoors in 0.3 m × 0.4 m × 0.1 m white plastic containers until reaching 3 % moisture content before being placed in the wind tunnel.

### 2.3 Wind-Tunnel Simulation Conditions

When simulating dust-emission processes, the shear stress produced by the airflow in the wind-tunnel boundary layer should be similar to that produced under field conditions, according to the objectives of the study (Van Pelt et al. 2010). Average threshold wind speed for soil wind erosion at 10 m is 8 m $s^{-1}$ (Hagen et al. 1999). The wind tunnel was run at two speeds, and as calculated by extrapolation of the average logarithmic wind profiles measured in the wind-tunnel working section (Fig. 3) these wind speeds produce shear stresses similar to the shear stress exerted on bare soils by wind speeds of 9.6 and 11.7 m $s^{-1}$ at the standard 10-m height. These wind speeds are similar to average wind speeds observed frequently in agricultural regions during dust storms. The wind tunnel was adjusted to obtain the corresponding friction velocities ($u_*$) of 0.2 and 0.3 m $s^{-1}$ respectively, similar to friction velocities reported by Kjelgaard et al. (2004) for PM10 emission under field conditions during high wind events. Friction velocities of about 0.2 m $s^{-1}$ can entrain particles of diameter about 75 μm into the saltation layer (Grini et al. 2002).

### 2.4 Sample Arrangement

The soil samples were transferred by hand from the plastic containers to a 0.2-m wide, 4-m long and 0.05-m deep metal tray located along the centre of the wind-tunnel working section (the soil bed). Once placed in the tray, the sample was leveled up by hand, sweeping it with a rod, to exactly match the level of the tunnel floor. The rest of the working section surface was lined with coarse emery cloth to imitate the surface roughness of the soil sample (Fig. 4a, b). Excess sample was removed from the sides of the soil bed using a brush.

**Table 1** Particle-size distribution of samples from the three different surfaces submitted to high and low wet dispersion procedures

| Size class* | Surface | | | | | | | | | |
|---|---|---|---|---|---|---|---|---|---|---|
| | | Sandy loam soil | | | Loamy sand soil | | | Unpaved road | | |
| | μm | Low dispersion | High dispersion | Ratio | Low dispersion | High dispersion | Ratio | Low dispersion | High dispersion | Ratio |
| Long suspensión | <2.5 | 1.9 | 4.4 | 2.31 | 1.2 | 5.6 | 4.67 | 0.8 | 2 | 2.5 |
| | <10 | 5.8 | 12.7 | 2.18 | 3.8 | 15.3 | 4.02 | 2.1 | 4.9 | 2.33 |
| | <20 | 9.58 | 18.88 | 1.97 | 7.1 | 22.51 | 3.16 | 3.32 | 6.74 | 2.03 |
| Short suspension | 20–50 | 8.64 | 10.42 | 1.26 | 11.13 | 12.33 | 1.1 | 2.89 | 3.31 | 1.14 |
| | 50–75 | 13.23 | 12.11 | 1.09 | 13.14 | 10.55 | 0.8 | 8.76 | 8.57 | 0.98 |
| Saltation | 75–500 | 67.97 | 57.96 | 0.85 | 68.03 | 53.37 | 0.78 | 74.94 | 75.62 | 1.01 |
| Reptation and creep | >500 | 0.58 | 0.63 | 1.08 | 0.6 | 1.24 | 2.06 | 10.1 | 5.78 | 0.57 |
| Saltation/PM10 ratio | | 11.7 | 4.5 | 2.6 | 17.9 | 3.5 | 5.1 | 35.7 | 15.4 | 2.3 |

The method used is laser diffraction analysis. The percentages refer to the number of particles within each size range
* Classified according to Kok et al. (2012)

**Table 2** Organic matter content (OM), erodible fraction (EF), and dry structural stability (DSS) of the analyzed surfaces

| | Surface | | |
|---|---|---|---|
| | Loamy-sand soil | Sandy-loam soil | Unpaved road |
| OM (%) | 1.3 | 2 | 0.7 |
| EF (%) | 62.5 | 82.6 | 94.0 |
| DSS (%) | 84.5 | 71.8 | 83.6 |

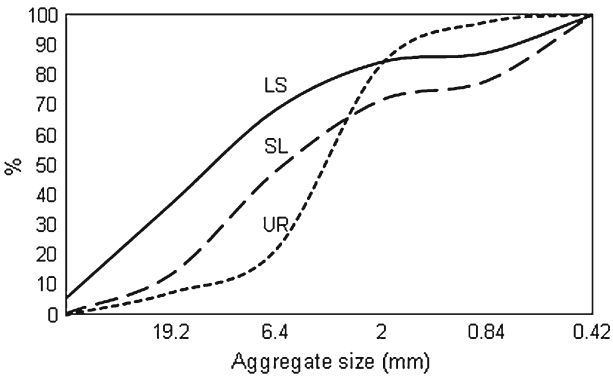


**Fig. 2** Aggregate size cumulative distribution of the analyzed surfaces (percentage mass) obtained with the rotary sieve method. *LS* loamy-sand soil, *SL* sandy-loam soil, *UR* unpaved road

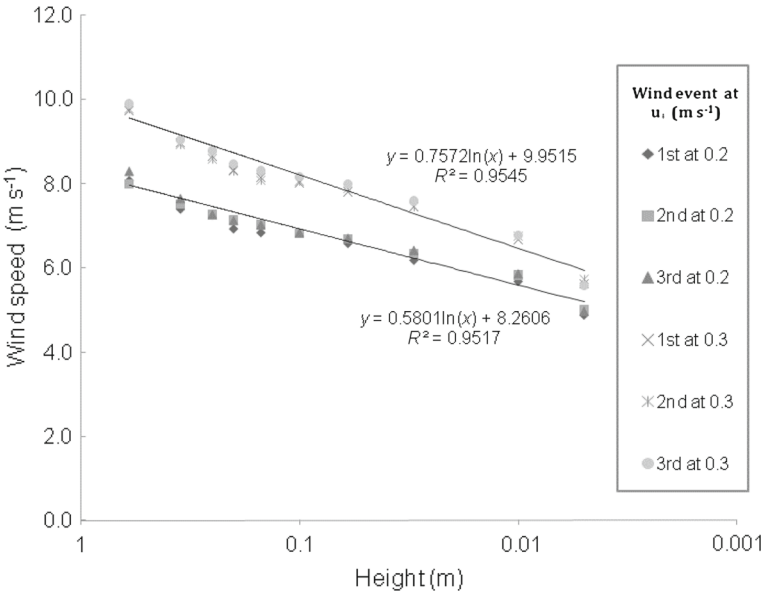


**Fig. 3** Average logarithmic wind profiles observed during consecutive wind events. Presented values were obtained averaging the three repetitions

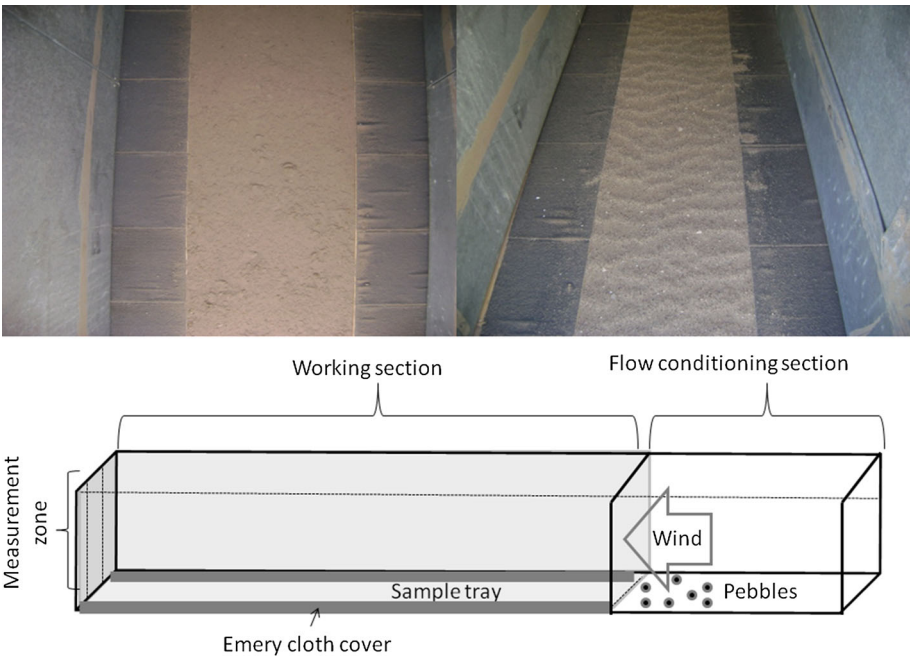


**Fig. 4** Condition of the soil bed of the sandy loam (*left*) soil and the unpaved road (*right*) after a 30-min wind simulation. The scheme shows the location of the sample tray and measurement zone

Natural limestone pebbles of 30–50 mm in diameter were randomly arranged but evenly spaced over a 1-m section on the floor of the clean section directly before the soil bed. This allowed the simulation of natural airflow turbulence before the soil bed. A scheme of the wind-tunnel set-up is shown in Fig. 4.

### 2.5 PM10 Emission and Horizontal Mass Transport

The Kanomax digital dust monitor measures the concentration of particles of diameter between 0.1 and 10 μm; the Kanomax 3442 model has a flow rate of 1 l $min^{-1}$ and a measurement range from 0.001 to 10 mg $m^{-3}$. PM10 concentrations were measured with a Kanomax 3442 digital dust monitor at ten different heights: 0.005; 0.01; 0.03; 0.06; 0.1; 0.15; 0.2; 0.25; 0.35 and 0.6 m at the exit of the wind tunnel. A metal probe 1.2-m long and 7-mm inside diameter was connected to the digital dust monitor, strapped alongside a pressure anemometer. This set was inserted vertically at the end of the wind tunnel and moved upwards at 1-min intervals from the beginning of the simulation, according to the above-mentioned heights. Measurements of PM10 concentrations and wind speeds were taken simultaneously during a 1-min period at each of the 10 heights. The digital dust monitor was programmed to take 10 samples of the PM10 concentration, one every 6 s, these ten concentration values were averaged for obtaining one value for each height. Hence one vertical profile for both wind speed and PM10 concentration was obtained for each 10-min simulation, along with one total sediment flux value. Three 10-min simulations were made consecutively, with each 10-min period considered as a consecutive wind-erosion event. The entire 30-min simulation was replicated three times for each wind speed and surface studied; fresh material was

reloaded into the trays prior to every 30-min simulation and measurements started after a 30-s stabilization period. Although the first moments of the emission process may produce data of interest, stabilization periods from 10 s on were also used in similar studies (Roney and White 2006; Burri et al. 2011) because they are necessary for avoiding the saturation of the measurement equipment and the great variability that is produced by the initial blow-off over some surfaces.

The simulation volume was located inside the wind-tunnel testing section, and defined as $W_b \times L_b \times H_t$, where $W_b$ and $L_b$ are the width (0.2 m) and the length (4 m) of the soil bed, and $H_t$ is the height (1 m) of the wind tunnel. The emission rate was defined as the mass emitted per unit area per unit time.

Since the aerosol sampler measures concentration, the downwind mass fluxes through the end of the working section were calculated from concentration and wind speed. The PM10 mass-flux rate per unit of vertical area (mg $m^2$ $s^{-1}$) at each sampling point at the exit of the simulation area ($PM10_f$) was defined as,

$$PM10_f = cu, \tag{1}$$

where $c$ is the PM10 concentration in mg $m^{-3}$ and $u$ is the wind speed in m $s^{-1}$. For an estimation of the material exiting the wind tunnel, the vertical mass-flux profile must be described. Power functions are the most prevalent for describing the vertical distribution of the dust mass flux (Hagen et al. 2010), and so the mass flux rate per unit of vertical area was calculated by fitting each $PM10_f$ value to a simple power function of the form

$$PM10_f(z) = az^b, \tag{2}$$

where $z$ is the height above the soil bed, and $a$ and $b$ are regression parameters ($b$ is negative). This function was then integrated to obtain the mass transport rate from the wind tunnel $M$ per unit width,

$$M = \int_{z_{min}}^{H_t} c_{(z)} u_{(z)} dz, \tag{3}$$

where $z_{min} = 0.005$ m is the lower integration limit and corresponds to the lowest measuring point over the soil surface, $H_t$ is the height of the wind tunnel. Integrating power functions towards zero height can produce overestimation of measured values because of function discontinuity near zero (Panebianco et al. 2010), hence measurements were taken as close as possible to the soil bed surface and this value was used as the lower limit of integration.

The emission rate $E$(kg $m^{-2}s^{-1}$) per unit of area of the soil bed was then calculated as

$$E = \frac{1}{L_b} \int_{z_{min}}^{H_t} c_{(z)} u_{(z)} dz. \tag{4}$$

As the mass fluxes at different heights through each sampling period are not entirely constant due to material depletion, a bias occurs in the vertical profile. But this disadvantage can only be avoided by using multiple measurement devices at different heights at the same time, provided they are perfectly calibrated with each other. The procedure used here is simpler, but PM10 vertical profiles are still scarce. This procedure was first introduced by Kim et al. (2000) and also used by Roney and White (2006). Although not perfect, the procedure used herein was also considered a good approach for describing the evolution of concentration profiles over time by McKenna Neuman et al. (2009). Moreover, similar approaches were

conducted more recently by Singh et al. (2012). Measurement periods are long enough to collect information at each height, but short enough to measure the entire profile during a relatively steady-state period. Furthermore, successive measurements are always made in the same way, so they remain comparable with one another. In the case that the PM10 flux is also registered at the entrance of the wind tunnel, a convenient mass balance can also be applied to this scheme (Roney and White 2006). As the measurements were made during clear atmosphere, low-wind-speed days, the background PM10 concentration values were very low. Hence PM10 concentrations at the entrance of the wind tunnel were negligible for the calculation procedures.

The total amount of material that is emitted per unit area of the soil bed $s^{-1}$, from hereafter the horizontal mass transport per unit area of the soil bed ($Q$), was measured at the end of the wind tunnel by means of four big spring number eight (Fryrear 1986) samplers placed at 0.06, 0.2, 0.35 and 0.6 m height measured to the centre of the sampler inlet. These samplers are extensively used in wind-erosion and dust-emission studies, especially for saltating, coarser material. However, their efficiency for catching particles of different sizes varies according to wind speed but they are considered to be effective for almost any size of particle (Goosens and Buck 2012) and their efficiency can also be compared to other type of samplers (Mendez et al. 2011). The amount of material trapped in the samplers was weighed after each 10-min simulation interval. Extra saltation material was not supplied to the soil bed. Sediment mass values collected in the samplers at each height were divided by the entrance area of each sampler for obtaining the mass fluxes $q$ per unit of vertical area in kg $m^{-2}$ $s^{-1}$ as follows,

$$q = \frac{m_i}{A_c T}, \tag{5}$$

where $m_i$ is the mass collected, $A_c$ is the area of the opening of the collector and $T$ is the duration of the sampling period. Exponential functions are widely used for describing the vertical profile of saltation mass flux (Panebianco et al. 2010), so the obtained mass fluxes at different heights were fitted to an exponential equation of the form,

$$q = ae^{-bz}, \tag{6}$$

where $q$ is the mass flux at height $z$, $a$ is the mass flux at height zero, and $b$ is a coefficient indicating the slope of the profile. Numerically integrating Eq. 6, the total sediment loss per unit time per unit width $Q$ is obtained. Analogous to the calculation of PM10 emission, the length of the soil bed ($L_b$) was used for finally obtaining $Q$ per unit bed area,

$$Q = \frac{1}{L_b} \int_0^{H_t} q_{(z)} dz, \tag{7}$$

where the height of the lower sampler inlet is zero, and $H_t$ is the height of the wind tunnel. This method of integrating the mass flux over the height has been widely used (Zobeck et al. 2003) and it is thoroughly reviewed in Panebianco et al. (2010).

The soil bed used was relatively narrow compared to the total area of the wind-tunnel floor and the measurements were made at the centre of the wind tunnel, where the main wind energy and mass flux occur. This may have resulted in a decreased particle concentration due to lateral diffusion. However, this issue is present in most of the wind-tunnel studies done to date using this methodology, and due to the uncertainties underlying every wind-tunnel study it is generally not considered a significant problem. The limited volume and the high erodibility of the tested surface can still produce an average particle concentration that can

be considered similar to that produced in the field under the same surface, fetch and wind conditions.

### 2.6 PM10 Emission Efficiency and Decay Rate

Vertical fluxes are generally estimated based on the concentration values measured at different heights (Gillette et al. 1997; Houser and Nickling 2001a; Whicker et al. 2014). Since the vertical dust flux is obtained through measurements made parallel to the airflow and to the soil surface, vertical fluxes, especially in a wind-tunnel environment, are very similar to horizontal fluxes (McKenna Neuman et al. 2009). This is because the flux inside the wind tunnel is predominantly horizontal due to the presence of walls and roof, so the estimates made about the vertical flux are in fact based on the horizontal flux. For this reason, we consider that the vertical flux (per unit bed area) of PM10 and the horizontal flux of PM10 (per unit bed area) at the end of the bed are the same because mass is conserved and PM10 re-deposits very slowly. Therefore, from now on we just refer to PM10 emission ($E$), without using the vertical or horizontal directions so as to avoid confusion.

The sandblasting efficiency was defined by Gillette (1978) for estimating the capacity of a surface to produce vertical dust flux,

$$F_{\mathrm{d}} = \alpha Q, \tag{8}$$

where $F_d$ is the vertical dust flux, $\alpha$ is the sandblasting efficiency, and $Q$ is the horizontal mass transport of particles (mainly saltation) per unit area of the soil bed (not per unit width). In a very similar way, here $\alpha$ represents the ratio of PM10 emission ($E$) and the total soil loss ($Q$) that is mainly composed of saltating particles from the wind tunnel,

$$\alpha = \frac{E}{Q}. \tag{9}$$

According to Shao (2008) the supply of particles for the saltation process is often limited, and for these cases we have

$$Q_{\mathrm{slm}} = \sigma \; Q \tag{10}$$

where $Q_{\mathrm{slm}}$ is the mass transport in a supply limited environment, and $Q$ is the mass transport under unlimited supply of particles, the potential saltation. The parameter $\sigma$ is dimensionless, and the evolution of $\sigma$ over time indicates the decay rate; note that $Q$is the mass transport value for the first wind-erosion events, considered as the potential saltation. As for each $Q$ value there is a corresponding $E$ value, and $\sigma$ was calculated as follows for both $Q$ and $E$,

$$\frac{Q_{\mathrm{slm}}}{Q} = \sigma_Q, \tag{11a}$$

$$\frac{E_{\mathrm{slm}}}{E} = \sigma_E, \tag{11b}$$

allowing us to obtain a measure of the decay rate of both the PM10 emission $E$ and the total soil loss rate $Q$ over the simulation time.

## 3 Results and Discussion

Table 1 shows the percentage of particles that are transportable by different mechanisms, and also shows the high dispersion to low dispersion ratio for each size fraction. If the

high dispersion to low dispersion ratio is >1 then particles in larger size ranges have a significant fraction of aggregates that, when broken up, increase the fraction of mass in the range in question. However if the high dispersion to low dispersion ratio is <1 then the size range in question has many aggregates that, when broken up, move to smaller size ranges. Of course only one of these mechanisms is possible for the extreme size ranges. The proportion of particles transportable by suspension was: loamy sand > sandy loam > unpaved road (as shown in Table 1). The ratio shows that the aggregation of the aggregates transportable by saltation was: loamy sand > sandy loam and unpaved road. The unpaved road had the highest proportion of particles transportable by saltation and these were mainly grains (high dispersion/low dispersion ratio close to 1, Table 1). The proportion of particles transportable by saltation was higher in the loamy sand than in the sandy loam (Table 1). The ratio between the high dispersion and the low dispersion treatments shows that a significant portion of the PM10 grains were located in aggregates coarser than 10 μm (because the mass of PM10 increases on break-up). The greater aggregation of the particles in the agricultural soils (sandy loam and loamy sand) compared to the unpaved road can be explained by differences in the organic matter content, which was: sandy loam > loamy sand > unpaved road (Table 2). Numerous studies have shown the positive effect of organic matter on soil aggregation (Mendez et al. 2006).

In the following sections the effects of the composition of the transported fraction concerning horizontal and vertical flows will be described.

### 3.1 PM10 Emission and Total Mass Transport

PM10 emission values ($E$) found varied between $12 \times 10^{-5}$ and $51 \times 10^{-4}$ kg m$^{-2}$ h$^{-1}$. $E$ values found in the literature are variable, e. g. Singh et al. (2012) found values between $1 \times 10^{-5}$ and $12 \times 10^{-3}$ kg m$^{-2}$ h$^{-1}$, while values ranged within $3 \times 10^{-5}$ and $89 \times 10^{-3}$kg m$^{-2}$ h$^{-1}$ at Owens lake (Roney and White 2006), and between $7 \times 10^{-3}$ and $50 \times 10^{-3}$ kg m$^{-2}$ h$^{-1}$ at the Mojave desert (Sweeney et al. 2011). In the sand plains of Iceland measurements averaged $35 \times 10^{-3}$ kg m$^{-2}$ h$^{-1}$(Thorsteinsson et al. 2011), and values around $36 \times 10^{-2}$ to $360 \times 10^{-3}$ kg m$^{-2}$ h$^{-1}$ were reported by Kim et al. (2000). These results were obtained under very different surface conditions and wind speeds, but they are useful in showing that the results found herein are within the range of PM10 emission values found in other regions of the world, though $E$ values expressed per unit of area of soil surface are not very frequent in the literature.

The unpaved road produced the highest horizontal mass transport ($Q$) and vertical flux ($E$), as shown in Fig. 5. Similar results were found by Feng et al. (2011) and Sweeney et al. (2011), who demonstrated that surfaces with low silt contents, such as sand dunes and sandy surfaces, can also be high PM10 emitters. Houser and Nickling (2001b) also found that absolute PM10 emission is linearly proportional to the horizontal mass transport; Kjelgaard et al. (2004) reported similar findings for field conditions.

Figure 5 shows changes for $Q$ and $E$ over successive wind-erosion events in the studied surfaces. The unpaved road produced high $Q$ and $E$ values but the amounts decreased rapidly in the second event. McKenna Neuman et al. (2009) also found a strong temporal variation of PM10 emission with particle supply limitation. Table 3 shows the coefficients of variation ($CV$) for each successive event ($n = 3$).

For a better comprehension of the $Q$ and $E$ changes in successive wind-erosion events, the values of the parameter $\sigma$ described by Shao (2008) are presented in Table 4. The $\sigma$ values for $E$ and $Q$ are indices of the fractional decrease of both variables as a function of the successive wind-erosion events that, according to Shao (2008), indicates the exhaustion

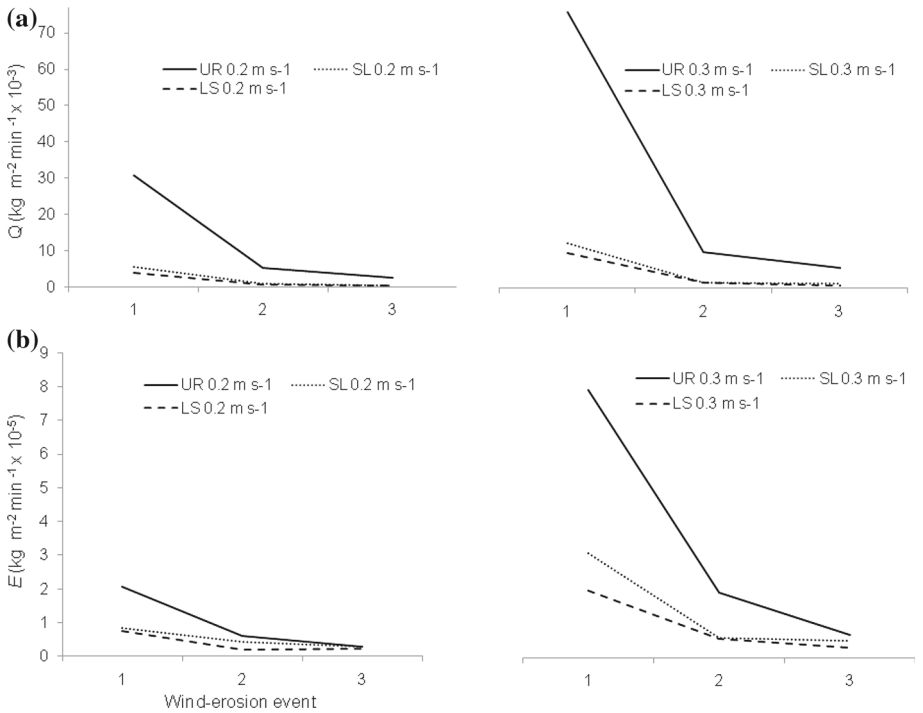


**Fig. 5** Changes in $Q$ (**a**) and $E$ (**b**) rates during three successive wind events at three surfaces and two different friction velocities. Values are given in scientific notation

**Table 3** Coefficients of variation ($CV$) calculated for each consecutive 10-min run during the measurement of $Q$ and $E$ ($n = 3$) from each studied surface (LS, SL and UR)

| Treatment/surface | | LS | | SL | | UR | |
|---|---|---|---|---|---|---|---|
| Run (10 min) | $u_*$ (m s$^{-1}$) | $Q$ | $E$ | $Q$ | $E$ | $Q$ | $E$ |
| 1 | 0.2 | 0.25 | 0.21 | 0.25 | 0.62 | 0.41 | 1.00 |
| 2 | 0.2 | 0.33 | 0.47 | 0.32 | 0.65 | 0.37 | 0.37 |
| 3 | 0.2 | 0.21 | 0.02 | 0.20 | 0.46 | 0.16 | 0.05 |
| 1 | 0.3 | 0.16 | 0.35 | 0.04 | 0.16 | 0.84 | 0.53 |
| 2 | 0.3 | 0.11 | 0.29 | 0.10 | 0.64 | 0.61 | 0.74 |
| 3 | 0.3 | 0.10 | 0.52 | 0.41 | 0.55 | 0.71 | 0.67 |

of the particles that can be mobilized. The parameter $\sigma$ indicates that $Q$ values decreased rapidly in the second successive wind-erosion event on all surfaces, being only 13–17 % of the amount registered during the first simulated wind-erosion event. Similar trends were detected at both wind speeds. However, $E$ values showed lower relative decreases than $Q$ values in the second wind-erosion event, and lower decreases for the lowest wind speed (25–51 % of the initial amounts) than for the highest wind speed (19–28 % of initial amounts), as shown in Table 4.

**Table 4** Values of the parameter $\sigma$ (Shao 2008) of $Q$ and $E$, as a function of the duration of the wind erosion event in three different surfaces

| Friction velocity ($m\ s^{-1}$) | Wind erosion event ($\times 10$ min) | $Q$ | | | $E$ | | |
|---|---|---|---|---|---|---|---|
| | | LS | SL | UR | LS | SL | UR |
| 0.2 | 1 | 1.00 | 1.00 | 1.00 | 1.00 | 1.00 | 1.00 |
| | 2 | 0.17 | 0.15 | 0.17 | 0.25 | 0.51 | 0.30 |
| | 3 | 0.13 | 0.09 | 0.09 | 0.29 | 0.40 | 0.14 |
| 0.3 | 1 | 1.00 | 1.00 | 1.00 | 1.00 | 1.00 | 1.00 |
| | 2 | 0.15 | 0.14 | 0.13 | 0.28 | 0.19 | 0.24 |
| | 3 | 0.08 | 0.11 | 0.07 | 0.16 | 0.17 | 0.09 |

The $Q$ values in the third successive wind-erosion event were between 7 and 13 % of the amount registered during the first simulated event, with similar trends at both wind speeds. $E$ values showed lower relative decreases than $Q$ values in the third wind-erosion event, with values between 14 and 40 % at the lower wind speed and between 9 and 17 % of the initial amounts at the higher wind speed (Table 4).

The values of the parameter $\sigma$ showed that $E$ was more sustained in successive wind-erosion events than $Q$. On the other hand, $Q$ showed similar trends in all the analyzed surfaces at both wind speeds while $E$ values showed a different behaviour at different wind speeds. Emission from agricultural soils was sustained in successive wind-erosion events due to the higher content of PM10 in particles of different sizes and densities, which are available for entrainment during longer time periods because they are depleted in successive erosion phases (Grini et al. 2002). In the coarser, non-aggregated, and more uniform unpaved road, PM10 particles are loose or slightly bonded to sand grains, and hence are rapidly depleted in direct relation to the saltation process. These differences in PM10 content and availability for aeolian entrainment can also produce changes over successive wind-erosion events concerning the sandblasting efficiency.

### 3.2 Sandblasting Efficiency ($\alpha$)

Values of $\alpha$ varied between $7 \times 10^{-5}$ and $67 \times 10^{-4}$ for the first event on the unpaved road at 0.2 m $s^{-1}$ and for the third event on the sandy loam at 0.2 m $s^{-1}$ respectively (Fig. 6). According to several studies, sandblasting efficiency values are around $10^{-5}$ to $10^{-2}$(Kok et al. 2012), while $\alpha$ values were higher in both agricultural soils than in the unpaved road. These results can be explained by the ratios between the saltation fraction content and the fine particulate matter (PM10) content of each surface (Table 1): these values were ordered in the sequence sandy loam < loamy sand << unpaved road. Agricultural soils, with lower saltation fraction to PM10 content ratios, presented higher $\alpha$ values due to the higher amount of PM10 available for entrainment per saltating particle. According to Alfaro and Gomes (2001), the saltation efficiency increases with the amount of PM20 (particulate matter with a mean aerodynamic diameter less than 20 $\mu$m) particles that are aggregated to form saltation particles. The same statement can be made analogous to the PM10 content. However, despite the loamy sand having a higher PM10 content, loamy sand has a lower saltation efficiency than sandy loam. This can be explained by the higher dry structural stability of the aggregates present in the loamy sand (Table 2).

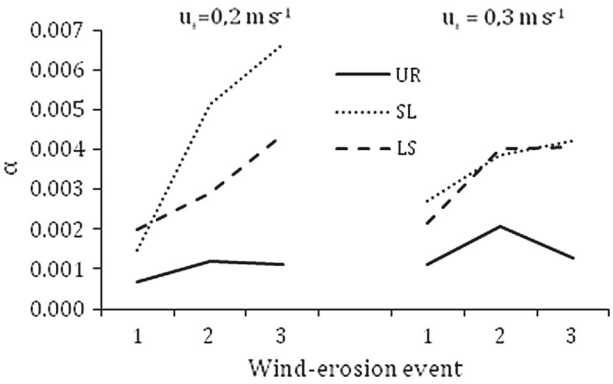


**Fig. 6** Sandblasting efficiency variation ($\alpha$) at two friction velocities as a function of wind blowing time in three different surfaces: loamy-sand soil (LS), sandy-loam soil (SL), and unpaved road (UR)

Figure 6 shows that, on the less aggregated surface such as the unpaved road, the saltation efficiency remains relatively constant during subsequent wind-erosion events as compared to the agricultural soils, which showed an increase of the efficiency in the successive events, especially for low friction velocity. These differences in the emission efficiencies between surfaces in successive events may help explain why some studies have found that saltation efficiency remains constant over time at different wind speeds, while other studies have found that efficiency changes with time and wind speed (Kok et al. 2012).

The saltation efficiency, generally symbolized by $\alpha$, has been controversial because of divergent results (Kok et al. 2012). Some authors have considered this parameter as being relatively constant (Gillette et al. 1997) for similar surfaces. Houser and Nickling (2001a) also found that vertical PM10 emission is not a function of the friction velocity in supply-limited environments and considered that supply limitation was the cause of the low correlation between wind speed and PM10 emission. Our results also suggested changes in the sandblasting efficiency for the same soil in successive wind-erosion events.

Agricultural soils (sandy loam and loamy sand) showed a tendency to increase their emission efficiency in successive wind-erosion events, as saltation diminished. Kjelgaard et al. (2004) reported that PM10 emission occurred even under very low saltation activity over agricultural soils under field conditions. Over the agricultural soils, a lower saltation fraction to PM10 content ratio, a higher content of PM10 and a higher aggregation of these PM10 particles (see high/low dispersion ratio for PM10 particles in Table 1) made it possible for the sandblasting efficiency to be sustained over a longer period of time than in the surface with low PM10 content and lower aggregation of PM10 particles (unpaved road). Over sandy surfaces, as with the unpaved road, intensive saltation activity is needed to produce proportional amounts of PM10. This apparent dependency of the sandblasting efficiency on the saltation fraction to PM10 content ratio and the aggregation condition of PM10 particles could help explain variations or oscillations in sandblasting efficiency found in previous studies, both in wind-tunnel and field conditions (Kok et al. 2014).

Results found here suggest that the condition of the PM10 particles in the soil affects the changes in the sandblasting efficiencies in successive wind-erosion events. Soils with PM10 particles contained within the aggregates, such as agricultural soils, showed important changes in the sandblasting efficiencies in successive wind-erosion events, while soils with loose PM10 particles, such as the unpaved road, showed less changes in the sandblasting effi-

ciencies over successive wind-erosion events. In the latter case, there is reasonable evidence to consider that the saltation efficiency remains relatively constant. However, in agricultural soils that are better structured and that contain PM10 particles forming aggregates, assuming a constant saltation efficiency in successive wind-erosion events or even during a single event can be misleading. The emission of PM10 during successive wind-erosion events can be underestimated when considering the saltation efficiency to be constant, as it is usually done when calculating the PM10 flow as a direct outcome from saltation.

Results suggest that the fragmentation produced during saltation or even creep of the particles can produce significant quantities of PM10 in sandy agricultural soils, but this is not likely to occur in sandier surfaces such as sand deserts or unpaved roads, where saltation at higher wind speeds should be necessary to produce significant entrainment of the PM10 particles attached to the sand grains. More studies are needed to better understand this process, but several insights are provided in the following section.

### 3.3 PM10 Vertical Entrainment

The PM10 concentration across the height range found here was described by a power-law function (Fig. 7), and is consistent with the vertical mass-distribution profiles described by other authors for the dust fraction (Sterk and Raats 1996). Exponential curves have also been reported for PM10 under field conditions and at higher sampling heights (McGowan and Clark 2008). The PM10 concentration under similar wind-tunnel conditions and calculation methods was previously evaluated by Kim et al. (2000) and Roney and White (2006), but changes in successive wind-erosion events were never considered. Figure 7 shows changes

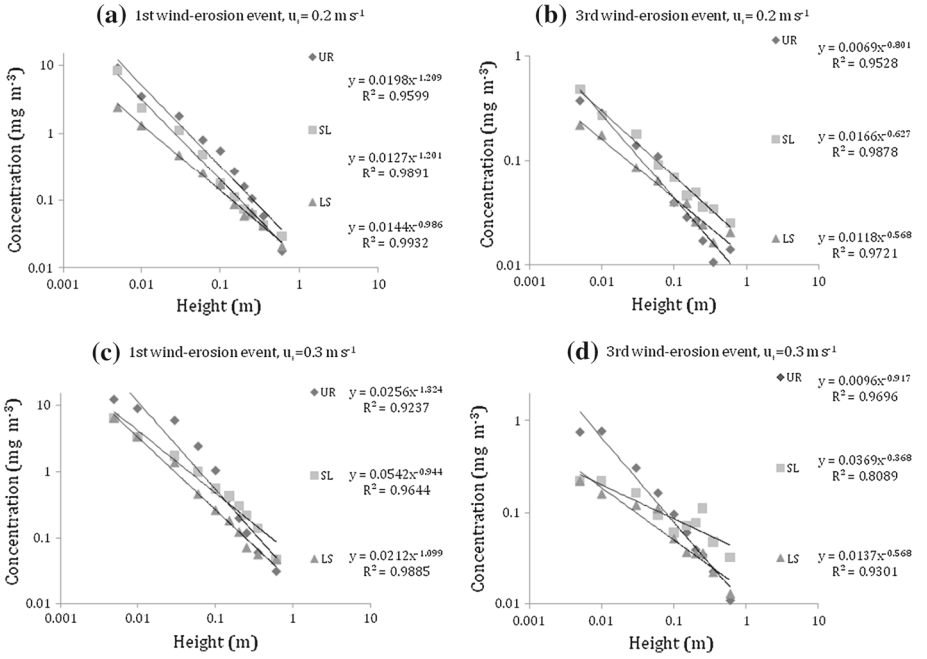


**Fig. 7** Double logarithmic plots showing the vertical distribution of the PM10 concentration during the simulation of the first (**a** and **c**) and the last (**b** and **d**) wind-erosion events

observed in the vertical distribution of PM10 concentration between the first and the last wind-erosion events.

According to Shao (2008), suspension depends on the relation between the terminal velocities of the particles and the airflow characteristics. Hence, suspension must differ between surfaces, and should also exhibit changes during successive wind-erosion events according to material availability on the eroded surface. An interesting point was that concentration values at 0.6 m were higher for agricultural soils than for the unpaved road, especially in the third wind-erosion event. This was due to the higher efficiency of the soils for producing fine particles that are easily entrained into the boundary layer of the wind tunnel; this is consistent with the saltation fraction to PM10 content ratios presented above. Greater vertical entrainment over agricultural soils was present at simulated higher wind speeds. On the sandier unpaved road, most of the PM10 particles were concentrated near the surface because of the low PM10 available for entrainment at the end of the wind tunnel. The fetch of the wind tunnel was 4 m; if the tested surface is a high efficiency PM10 emitter, the vertical profile will be developed earlier (at a shorter distance from the beginning of the soil bed). But on a sandier surface, a greater distance is needed to produce enough saltation activity to release the PM10 and produce a more developed vertical profile (or dust plume). This effect was even more evident after the second successive wind-erosion event because of the higher dependency of the PM10 emission on the saltation process on the sandier surface, as discussed previously (Fig. 7).

No evidence of significant alteration of wind-speed profiles was observed (Fig. 3). Therefore, these results show that changes in the composition of the surface erodible layer during a high wind event can also produce important changes in the entrainment patterns. This effect, along with the heating of the soil surface (Butler et al. 2005), could help to explain the variable concentration profiles observed under field conditions (Kjelgaard et al. 2004). The question of how this dynamical process affects the theoretical schemes or predictions made with emission models needs further investigation.

## 4 Conclusions

PM10 emissions were measured on material from two typical agricultural soils and a typical dirt road from central Argentina. A wind tunnel was used for testing the surfaces under high wind speeds and high emissivity conditions during three consecutive 10-min intervals. High saltation rates (horizontal mass transport, $Q$) produced high PM10 emissions, independent of the PM10 bulk content or the emission efficiency of the surface. Unpaved roads showed the highest saltation rates. Considering that they are permanently bare (an absence of vegetation cover), and they have long upwind fetches, unpaved roads can be sources of atmospheric dust and PM10 emission in rural areas during high wind events, especially those aligned with the prevailing wind direction.

Horizontal mass transport decreased at similar rates in successive wind-erosion events on all analyzed surfaces; nevertheless, the decrease in PM10 emission was more rapid in the unpaved road than in the agricultural soils. Sandblasting efficiency increased in successive wind-erosion events in the agricultural soils. Sandblasting efficiency for PM10 emissions was higher for the agricultural soils than for the unpaved road, particularly at lower wind speeds, because of the higher PM10 content of soil aggregates.

Vertical concentration profiles were different over different surfaces and also evolved in different ways during the wind event. On the unpaved road, PM10 concentrations at

a fetch of 4 m rapidly decreased with height while agricultural soils showed higher PM10 vertical entrainment, especially at high wind speeds and after successive wind-erosion events. These results suggest that the sandblasting efficiency for PM10 emission and vertical PM10 concentration profiles is influenced by the duration of the wind-erosion event, and that the ratio of saltation fraction to PM10 content of the surface material can be a simple indicator of this trend. Temporal dynamics help explain some of the variability found under field conditions and improve theoretical schemes and model prediction, but further studies are needed.

## References


Aimar S, Mendez M, Funk R, Buschiazzo DE (2012) Soil properties related to potential particulate matter emissions (PM10) of sandy soils. Aeolian Res 3:437–443

Alfaro SC, Lopez MV, Sabre M, Gomes L (1998) Implications of a sandblasting model for dust production by wind erosion in arid areas. In: Wind Erosion: an international symposium commemorating the 50th anniversary of the USDA's wind erosion research at Kansas State University, Manhattan, Kansas, USA

Alfaro SC, Gomes L (2001) Modelling mineral aerosol production by wind erosion: emission intensities and aerosol size distributions in source areas. J Geophys Res 106:18075–18084

Baddock MC, Zobeck TM, Van Pelt RS, Fredrickson EL (2011) Dust emissions from undisturbed and disturbed, crusted playa surfaces: Cattle trampling effects. Aeolian Res 3:31–41

Burri K, Gromke C, Lehning M, Graf F (2011) Aeolian sediment transport over vegetation canopies: a wind tunnel study with live plants. Aeolian Res 3:205–213

Buschiazzo DE, Aimar S, Zobeck TM (1999) Wind erosion in soils of the semiarid Argentinian Pampas. Soil Sci 164:133–138

Butler HJ, McTainsh GH, Hogarth WL, Ley JF (2005) Kinky profiles: effects of soil surface heating upon vertical dust concentration profiles in the Channel Country of western Queensland, Australia. J Geophys Res 110:1–14

Carvacho OF, Ashbaugh LL, Flocchini RG (2006) Elemental composition of PM10 and PM2.5 in ambient air downwind of agricultural operations in California's San Joaquin Valley. In: Brebbia, CA et al. (Eds.), Management of Natural Resources, Sustainable Development and Ecological Hazards (The Ravage of thePlanet 2006). Witpress.com, Southampton. doi:10.2495/RAV110171

Dockery DW, Pope CA (1994) Acute respiratory effects of particulate air pollution. Annu Rev Public Health 15:107–132

Etyemezian V, Kuhns H, Gillie J, Green M, Pitchford M, Watson J (2003) Vehicle-based road dust emission measurement: methods and calibration. Atmos Environ 37:4559–4571

Feng G, Sharratt B, Wendling L (2011) Fine particle emission potential from loam soils in a semiarid region. Soil Sci Soc Am J75:2262–2270

Fryrear DW (1985) Determining soil particle stability with a rapid rotary sieve. J Soil Water Conserv 40:231–233

Fryrear DW (1986) A field dust sampler. J Soil Water Conserv 41:117–120

Gee GW, Bauder JW (1986) Particle-size analysis. In: Klute A (ed) Methods of soil analysis, vol 5., Soil Science society of America Book SeriesSoil Science society of America, Madison, pp 383–411

Gillette DA (1978) A wind tunnel simulation of the erosion of soil: effect of soil texture, sandblasting, wind speed, and soil consolidation on dust production. Atmos Environ 12:1735–1743

Gillette DA, Fryrear DW, Gill TE, LeyT Cahill TA, Gearhart EA (1997) Relation of vertical flux of grains smaller than 10 $\mu$m to total aeolian horizontal mass flux at Owens Lake. J Geophys Res 102:26009–26015

Goossens D, Buck B (2009) Dust emission by off-road driving: experiments on 17 arid soil types, Nevada, USA. Geomorphology 107:118–138

Goossens D, Buck B (2011) Effects of wind erosion, off-road vehicular activity, atmospheric conditions and the proximity of a metropolitan area on PM10 characteristics in a recreational site. Atmos Environ 45:94–107

Goosens D, Buck B (2012) Can BSNE (Big Spring Number Eight) samplers be used to measure PM10, respirable dust, PM2.5 and PM1.0? Aeolian Res 5:43–49

Grini A, Zender CS, Colarco PR (2002) Saltation sandblasting behaviour during mineral dust aerosol production. Geophys Res Lett 29(18):1868. doi:10.1029/2002GL015248

Hagen LJ, Wagner LE, Skidmore EL (1999) Analytical solutions and sensitivity analyses for sediment transport in WEPS. Trans ASAE 42:1715–1721

Hagen LJ, van Pelt S, Sharratt B (2010) Estimating the saltation and suspension components from field wind erosion. Aeolian Res 1:147–153
Harrison P, Kohfeld KE, RoelandtC Claquin T (2001) The role of dust in climate changes today, at the last glacial maximum and in the future. Earth Sci Rev 54:43–80
Houser CH, Nickling WG (2001a) The emission and vertical flux of particulate matter < 10 um from a disturbed clay-crusted surface. Sedimentology 48:255–267
Houser CH, Nickling WG (2001b) The factors influencing the abrasion efficiency of saltating grains on a clay-crusted playa. Earth Surf Process Landf 26:491–505
Kim DS, Cho GH, White BR (2000) A wind-tunnel study of atmospheric boundary-layer flow over vegetated surfaces to suppress $Pm_{10}$ emission on Owens (dry) lake. Boundary-Layer Meteorol 97:309–329
Kjelgaard J, Sharratt B, Sundram I, Lamb B, Claiborn C, Saxton K, Chandler D (2004) PM10 emission from agricultural soils on the Columbia Plateau: comparison of dynamic and time-integrated field-scale measurements and entrainment mechanisms. Agric For Meteorol 125:259–277
Kok JF, Parteli EJR, Michaels TI, Bou Karam D (2012) The physics of wind-blown sand and dust. Rep Progr Phys 75: 72 pp
Kok JF, Mahowald NM, Albani S, Fratini G, Gillies JA, Ishizuka M, Leys JF, Mikami M, Park MS, Park SU, Van Pelt RS, WardDS Zobeck TM (2014) An improved dust emission model with insights into the global dust cycle's climate sensitivity. Atmos Chem Phys Discuss 14:6361–6425
Liu Lian-You, Shi Pei-Jun, Zou Xue-Yong, Gao Shang-Yu, Erdon Hasi, Yan Ping, Li Xiao-Yan, Dong Zhi-Bao, Wang Jian-Hua (2003) Short-term dynamics of wind erosion of three newly cultivated grassland soils in Northern China. Geoderma 115:55–64
López MV (1998) Wind erosion in agricultural soils: an example of limited supply of grains available for erosion. Catena 33:17–28
Mahowald NM, Baker AR, Bergametti G, Brooks N, Duce RA, Jickells TD, Kubilay N, Prospero JM, Tegen I (2005) Atmospheric global dust cycle and iron inputs to the ocean. Glob Biogeochem Cycle 19:GB4025. doi:10.1029/2004GB002402
Marticorena B, Bergametti G (1995) Modeling the atmospheric dust cycle: 1. Design of a soil-derived dust emission scheme. J Geophys Res 100:16415–16430
McKenna Neuman Ch, Boulton JW, Sanderson S (2009) Wind tunnel simulation of environmental controls on fugitive dust emissions from mine tailings. Atmos Environ 43:520–529
McGowan HA, Clark A (2008) A vertical profile of PM10 dust concentrations measured during a regional dust event identified by MODIS Terra, western Queensland, Australia. J Geophys Res 113:1–10
McTainsh G, Strong C (2007) The role of aeolian dust in ecosystems. Geomorphology 89:39–54
Mendez MJ, de Oro L, Panebianco JE, Colazzo JC, Buschiazzo DE (2006) Organic carbon and nitrogen in soils of semiarid Argentina. J Soil Water Conserv 61:230–235
Mendez MJ, Funk R, Buschiazzo DE (2011) Field wind erosion measurements with big spring number eight (BSNE) and modified wilson and cook (MWAC) samplers. Geomorphology 129:43–48
Panebianco JE, Buschiazzo DE, Zobeck TM (2010) Comparison of different mass transport calculation methods for wind erosion quantification purposes. Earth Surf Process Landf 35:1548–1555
Roney JA, White BR (2006) Estimating fugitive dust emission rates using an environmental boundary layer wind tunnel. Atmos Environ 40:7668–7685
Sharratt B, Feng G, Wendling L (2007) Loss of soil and PM10 from agricultural fields associated with high winds on the Columbia Plateau. Earth Surf Process Landf 32:621–630
Shao Y (2008) Physics and modelling of wind erosion. Atmospheric and Oceanographic Sciences Library, Vol. 37, $2^{nd}$ edition. Springer, Netherlands 456 pp
Singh P, Sharrat B, Schillinger WF (2012) Wind erosion and PM10 emission affected by tillage systems in the world's driest rainfed wheat region. Soil Tillage Res 124:219–225
Sterk G, Raats PAC (1996) Comparison of models describing the vertical distribution of wind eroded sediment. Soil Sci Soc Am J 60:1914–191
Sweeney MR, McDonald EV, Etyemezian V (2011) Quantifying dust emissions from desert landforms, eastern Mojave Desert, USA. Geomorphology 135:21–34
Thorsteinsson T, Gísladóttira G, Bullard J, McTainsh G (2011) Dust storm contributions to airborne particulate matter in Reykjavík, Iceland. Atmos Environ 45:5924–5933
Van Pelt RS, Zobeck TM, Baddock MC, Cox JJ (2010) Design, construction and calibration of a portable boundary layer wind tunnel for field use. Trans ASABE 53:1413–1422
Walkley A, Black IA (1934) An examination of the Degtjareff method for determining soil organic matter, and a proposed modification of the chromic acid titration method. Soil Sci 37:29–38
Whicker JJ, Breshears DB, Field JP (2014) Progress on relationships between horizontal and vertical dust flux: Mathematical, empirical and risk-based perspectives. Aeolian Res 14:105–111

Zobeck TM, Sterk G, Funk R, Rajot JL, Stout JE, Van Pelt RS (2003) Measurement and data analysis methods for field-scale wind erosion studies and model validation. Earth Surf Process Landf 28:1163–1188. doi:10.1002/esp.1033

Zobeck TM, Van Pelt RS (2006) Wind-induced dust generation and transportmechanics on a bare agricultural field. J Hazard Mater 132:26–38